

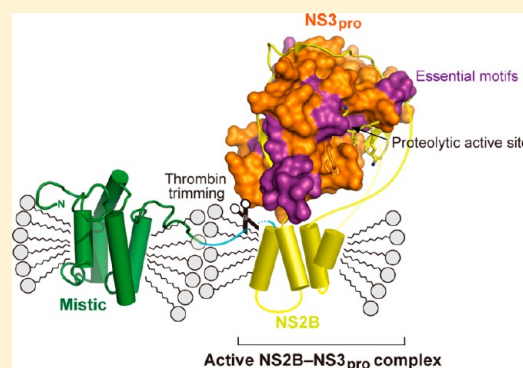
Structural Platform for the Autolytic Activity of an Intact NS2B–NS3 Protease Complex from Dengue Virus

Opas Choksupmanee, Kenneth Hodge, Gerd Katzenmeier, and Sarin Chimnarong*

Institute of Molecular Biosciences, Mahidol University, Salaya Campus, Phutthamonthon, Thailand 73170

S Supporting Information

ABSTRACT: Dengue virus completes its protein synthesis inside human cells on the endoplasmic reticulum membrane by processing the single-chain polypeptide precursor into 10 functional proteins. This vital process relies on the two-component virus-encoded protease complex; non-structural protein 3 (NS3) possesses the proteolytic activity in its N-terminus, and NS2B acts as a fundamental activator and membrane-anchoring subunit. The membrane-associated NS2B–NS3 complex has essentially not yet been isolated or studied. We describe here a useful protocol for the preparation of the full-length NS2B–NS3 complex from dengue serotype 2 virus by utilizing a Mistic-fusion expression cassette in *Escherichia coli*. The protease complex was successfully solubilized and stabilized from the bacterial membrane and purified with the use of fos-choline-14 detergent. The detergent-solubilized protease complex retained autolytic activity and, intriguingly, exists as a robust trimer, implying a molecular assembly in the membrane. We further conducted a random mutagenesis study to efficiently scan for entire residues and motifs contributing to autocleavage and provide evidence of the importance of the two distal β -hairpins in the activity of the viral protease. Our results provide the first comprehensive view of an active dengue protease in the membrane-bound form.



Dengue virus (DENV) is a mosquito-borne human pathogen that causes serious public health problems in tropical and subtropical regions around the world, with an estimated 50–100 million infections per year.¹ DENV cocirculates as a complex of four closely related but antigenically distinct serotypes (DENV-1–DENV-4), all of which are etiologic agents of dengue fever, and the life-threatening dengue hemorrhagic fever (DHF) and dengue shock syndrome (DSS).^{2,3} At present, there are neither effective vaccines nor antiviral drugs available to protect or cure dengue diseases, and the mechanisms involved in the pathogenesis of the disease remain largely unknown. DENV is a member of the genus *Flavivirus* within the family *Flaviviridae*, which comprises several medically important pathogens, including the Japanese encephalitis (JEV), yellow fever (YFV), and West Nile (WNV) viruses (for reviews, see refs 4 and 5). Like all flaviviruses, DENV is an enveloped virus possessing a positive-sense, single-strand RNA genome of approximately 10.7 kb that is translated as a single long polypeptide precursor ~3390 amino acids in length and proteolytically cleaved into 10 viral proteins: three structural (capsid, premembrane/membrane, and envelope) and seven nonstructural (NS1, NS2A, NS2B, NS3, NS4A, NS4B, and NS5) proteins.⁶ Accurate processing of the viral polypeptide is vital for virus replication and is achieved co- and post-translationally by a combination of cellular proteases, including signalase and furin, and the two-component virus-encoded serine protease (NS2B–NS3).^{7,8}

The NS3 protein is an ~69 kDa multifunctional enzyme containing a chymotrypsin-like serine protease module at its N-

terminus, whereas the C-terminal two-thirds of the protein are associated with RNA triphosphatase and NTPase/RNA helicase activities.^{9–11} The N-terminal protease domain of NS3 (NS3_{pro}) harbors a classical catalytic triad comprised of residues His⁵¹, Asp⁷⁵, and Ser¹³⁵ located at the cleft between the two constituent β -barrels.¹² Despite most fundamental architectures necessary for the protease activity comprising NS3 residues 1–180, the enzyme intrinsically requires the formation of a heterodimeric complex with cofactor protein NS2B to be mature and functionally active. Several lines of evidence revealed that the central 40-residue hydrophilic segment of NS2B (NS2B_H) is essential and sufficient for activation of the proteolytic activity of NS3_{pro} in vivo and in vitro.^{13–16} Hence, most biochemical and structural studies have so far focused only on NS2B_H peptide-linked NS3 constructs. These types of engineered protease complexes were expressed in soluble form by *Escherichia coli* and retained high *cis* and *trans* proteolytic activities.^{16,17} However, the question of whether these artificial constructs reflect the properties of the genuine protease complex in the membranous environment in infected cells remains highly controversial.^{18,19} It is likely that the membrane has considerable effects on the structure and activity of the NS2B–NS3 complex as suggested by an augmentation of the in vitro activity of the NS2B_H–NS3_{pro}

Received: December 11, 2011

Revised: March 1, 2012

Published: March 8, 2012



complex upon addition of zwitterionic and nonionic detergents.¹⁷

Dengue NS2B is a 130-amino acid (14 kDa) integral membrane protein that contains three putative hydrophobic transmembrane segments flanking the conserved NS2B_H activation center.²⁰ Notably, full-length NS2B could activate NS3_{pro} only in the presence of membrane lipids, thereby stimulating the membrane association of the NS3 protease.¹⁵ Recently, crystal structures of dengue NS2B_H complexed with full-length NS3 and NS3_{pro} have been determined at high resolution, suggesting that NS2B_H regulates the activity of NS3_{pro} by fine-tuning the secondary structure and stabilizing the active form of the NS3_{pro} protein as a molecular chaperone.^{12,21} However, NS2B_H fragments in these crystal structures showed a pattern of disorder and were located away from the active sites. It was therefore not possible to offer precise mechanisms for NS2B-dependent substrate recognition, proteolytic reaction, and membrane association of dengue NS3. In addition, the NS2B–NS3_{pro} complex apparently coordinates the RNA binding and ATPase activities of the neighboring C-terminal helicase domain of NS3 by precluding the DNA binding potentiality and optimizing the performance of the ATPase rate during RNA unwinding.^{21–24}

Because of its significance in the viral life cycle, and its idiosyncrasy and high degree of conservation across genotypes, the NS2B–NS3_{pro} complex is ideally suited to be a drug target for DENV therapeutics. To gain new insight into the structure and functional mechanisms of the membrane-associated dengue protease, we successfully utilized a protein fusion system for overexpression of the dengue protease complex in the *E. coli* membrane. The membrane-bound form of the dengue NS2B–NS3_{pro} complex was thoroughly purified and characterized in the presence of a solubilizing detergent. Our study represents a breakthrough in functional and structural studies of the intact NS2B–NS3 protease complex in the search for antiviral compounds.

■ EXPERIMENTAL PROCEDURES

Materials. The pETDuet-1 vector was obtained from Novagen (EMD Biosciences). Phusion DNA polymerase was purchased from Finnzymes (Espoo, Finland). *Pfu* DNA polymerase and restriction enzymes (*Nco*I, *Bam*HI, *Eco*RI, and *Hind*III) were obtained from Promega (Madison, WI). Fast Blast dye and gel filtration standard proteins were purchased from Bio-Rad (Hercules, CA). Detergents were purchased from Anatrace (Maumee, OH). Amicon concentration devices and Immobilon chemiluminescent HRP substrates were purchased from Millipore (Billerica, MA). His-probe (H-3)-HRP (mouse monoclonal IgG₁) was from Santa Cruz Biotechnology (Santa Cruz, CA). Thrombin protease and purification columns (His-Trap, Hi-Trap chelating column, RESOURCE Q, and Superdex 200 HR 10/30 gel filtration column) were purchased from GE healthcare (Buckinghamshire, U.K.). The other commonly used chemical reagents, including isopropyl 1-thio- β -D-galactopyranoside (IPTG), dithiothreitol (DTT), imidazole, phenylmethanesulfonyl fluoride (PMSF), dimethyl sulfoxide (DMSO), and glycerol, were obtained from Sigma-Aldrich (St. Louis, MO).

Construction of Protein Expression Vectors. The expression vector for the production of dengue NS2B–NS3 protease complexes was generated by a stepwise procedure. Initially, the *Mistic* gene from *Bacillus subtilis* was amplified from the genome via polymerase chain reaction (PCR) using

two specific oligonucleotide primers of 5'-CATGAC-CATGGGCTttttgtacatttttgaaaacatc-3' (sense) and 5'-GGTGATGATGTCCAGAACCTCCAGAGCCttttttctcttcagatac-3' (antisense), yielding a product of approximately 371 bp (the *Mistic* gene regions are indicated by lowercase letters, while restriction sites and overlapping sequences are italic and underlined, respectively). The resulting fragment also contained a six-amino acid linker (GSGGSG) followed by a part of the octahistidine tag (8×His). Subsequently, the remaining His tag, the GSSG linker, and the thrombin cleavage sequence were synthesized using two overlapping primers, 5'-GGTCTGGA-CATCATCACCATCATCATCACCACGGTTCTAGCG-GATTAG-3' and 5'-TGACGGATCCTGGCTA-GATCCGCGTGGCACTAATCCGCTAGAACCGTGG-3' (the thrombin sequence is bold). Eventually, both resulting fragments were combined via PCR ligation, taking advantage of overlapping sequences, and the complete insert was then digested, purified, and ligated into the pETDuet-1 vector between *Nco*I and *Bam*HI restriction sites upstream of the first multicloning site (MCS1), yielding the “pMHTD” vector. In the next stage, the full-length NS2B–NS3_{pro} gene from dengue virus serotype 2 strain 16681 was amplified from the virus cDNA plasmid as previously described with primers containing *Eco*RI and *Hind*III restriction sites and subsequently cloned into MCS1 of the pMHTD vector. Enzymatically inactive mutants with A1E and S135A exchanges in the NS3 sequence were generated by the QuikChange site-directed mutagenesis kit according to the manufacturer's protocol (Stratagene, La Jolla, CA). The identities of the recombinant constructs were confirmed by automated DNA sequencing.

Protein Expression and Detergent Solubilization. *E. coli* strain BL21(DE3) derivative, Rosetta 2 (Novagen, EMD Biosciences) cells were transformed with pMHTD-NS2B-NS3_{pro} (wild type, A1E, and S135A) vectors and grown in Luria-Bertani broth (LB) supplemented with a combination of ampicillin (100 μ g/mL), chloramphenicol (34 μ g/mL), and 1% glucose at 37 °C. After the culture reached an OD₆₀₀ of 0.5, production of the protein was immediately induced by addition of 0.1 mM IPTG and proceeded for an additional 6 h at 25 °C. Cells were harvested and disrupted by sonication in lysis buffer containing 50 mM Tris-HCl (pH 8.0), 1 mM EDTA, 10% glycerol, 250 mM NaCl, 7 mM β -mercaptoethanol, 0.5 mg/mL lysozyme, and 1 mM PMSF. Cell debris and large inclusion bodies were removed from the cell lysate by low-speed centrifugation prior to the collection of the membrane-containing pellet by ultracentrifugation at 100000g for 1 h at 4 °C.

The membrane fractions were homogeneously resuspended in lysis buffer deprived of lysozyme and treated with 1–2% detergents overnight at 4 °C to solubilize the membrane protein. The overall protein concentration was kept at a constant level during the extraction at 5 mg/mL as determined by the Bradford assay. Detergent-solubilized membrane protein fractions were separated from inclusion bodies by ultracentrifugation as described above and analyzed via a 12% sodium dodecyl sulfate–polyacrylamide gel stained with Coomassie Brilliant Blue-R250 and Western blotting.

Purification of the Dengue NS2B–NS3 Protease Complex. For large-scale purification, the dengue protease complex was extracted and solubilized with 1% fos-choline-14 (FC-14) (molecular mass of 379.5 Da) from the *E. coli* membrane at 4 °C. The clear supernatant obtained by ultracentrifugation at 100000g was directly loaded onto a Hi-

Trap chelating column equilibrated with washing buffer containing 50 mM Tris (pH 8.0), 150 mM NaCl, 25 mM imidazole, 10% glycerol, and 0.25% (w/v) FC-14. The column was washed with 20 column volumes of washing buffer, and bound proteins were eluted at a flow rate of 0.5 mL/min with 5 column volumes of elution buffer containing 250 mM imidazole. The fractions containing the tagged dengue protease were batched together and desalted using Amicon Ultra centrifugal filter units.

To remove all fusion tags from the desired protein, an adequate amount of the thrombin protease was added to the protein solution supplemented with 5 mM MgCl₂ and gently mixed at 4 °C. The digestion efficiency was monitored via SDS–PAGE, and the reaction was quenched by addition of 1 mM PMSF. We found that a certain quantity of thrombin up to 100 units/mg of protein was required to complete the digestion. Following tag removal, the immobilized affinity column (IMAC) procedure was repeated to separate untagged dengue protease from Mistic.

As we were not successful in suppressing the proteolytic activity of the wild type NS2B–NS3_{pro} complex during the purification, the S135A mutant was exclusively subjected to further purification steps to increase the sample purity. The affinity-purified protein solution was adjusted to pH 7.0 in AE buffer [25 mM HEPES (pH 7.0), 10% glycerol, 1 mM DTT, and 0.1% FC-14], subsequently applied to an anion exchange RESOURCE Q column pre-equilibrated with AE buffer containing 25 mM NaCl, and eluted with a linear gradient from 25 to 300 mM NaCl. The NS2B–NS3_{pro} complex eluted at approximately 180 mM NaCl and was pooled and concentrated using a 10 kDa molecular mass cutoff Amicon Ultra-4 device. The final step of purification was performed using a Superdex 200 HR 10/30 gel filtration column on an Äkta Purifier FPLC system (GE Healthcare). The pure NS2B–NS3_{pro} complex was eluted from the column at a flow rate of 0.5 mL/min with 24 mL of GF buffer comprised of 25 mM HEPES (pH 7.6), 100 mM NaCl, 10% glycerol, 1 mM DTT, and 0.1% FC-14. The homogeneity of the purified protein was assessed via SDS–PAGE. The molecular mass of NS2B–NS3_{pro}–detergent complexes was estimated by calibrating the column with a gel filtration standard mixture. The molecular mass was correlated to retention volume by using a power law curve fit.

Western Blot Analysis. The protein fractions containing the NS2B–NS3 protease complex were separated via 12% SDS–PAGE and subsequently transferred to a nitrocellulose membrane. After being treated with blocking solution (1% skim milk and 0.1% Tween 20 in PBS) for 1 h at room temperature, the blots were incubated with an anti-His tag (1:1000, Santa Cruz) or anti-NS3_{pro} antibodies for 1 h at room temperature. To visualize the protein bands of interest, the membrane was incubated with rabbit anti-mouse immunoglobulin coupled to a streptavidin–horseradish peroxidase conjugate for 1 h at room temperature and colorimetrically detected by diaminobenzidine (DAB).

Secondary Structure Analysis by Circular Dichroism (CD) Spectroscopy. CD spectra were recorded with a Jasco J-715 CD spectropolarimeter (Jasco Corp.) at ambient temperature over UV wavelengths of 190–250 nm with a step size of 1 nm and an averaging time of 1 s. The protein concentration was fixed at 0.5 mg/mL in GF buffer. Spectra shown for the purified NS2B–NS3_{pro} complex were blanked against GF buffer to remove effects of detergent FC-14. The spectra were analyzed

with CDPro algorithms (<http://lamar.colostate.edu/~sreeram/CDPro/main.html>).

Protein Cross-Linking. Three to five micrograms of the gel-purified NS2B–NS3_{pro} complex (S135A) was pulsed with an increasing concentration of a glutaraldehyde solution (Electron Microscopy Sciences) from 0 to 0.5%, or 0.25 mM disuccinimidyl suberate (DSS) (Thermo Fisher Scientific). The 10 µL reaction mixtures were incubated in the dark at 25 °C for 2 and 30 min for glutaraldehyde and DSS, respectively, and the reactions subsequently quenched with 50 mM Tris–HCl (pH 8.0) for 15–20 min. Cross-linked proteins were separated by 8% SDS–PAGE under reducing conditions followed by silver staining (GE healthcare).

Blue Native Polyacrylamide Gel Electrophoresis (BN–PAGE). Electrophoresis was performed according to Invitrogen's instructions. In brief, typical unheated sample mixtures (10 µL) contained 50 mM Bis–Tris, 50 mM NaCl, 10% glycerol, 0.001% Ponceau S, 0.025% Commassie G-250, 0.1% FC-14, and pure S135A proteins (1–7.5 µg). After a short incubation at room temperature, the solutions were loaded onto 4 to 16% precast gradient Novex Bis–Tris gels (Invitrogen) with a running buffer containing 50 mM Bis–Tris (pH 6.8) and 50 mM Tricine. BN gels were run at a constant voltage of 150 V at room temperature for 105–120 min until the dye front migrated to the gel bottom. For molecular mass standards, wide-range NativeMark markers (Invitrogen) were used.

Random Mutagenesis of the NS2B–NS3_{pro} Complex.

A library of NS2B–NS3_{pro} variants was generated using the GeneMorph II EZClone domain mutagenesis kit (Stratagene) with two specific primers: forward, 5'-AGCTGGCCAT-TAAATGAGGCTATCATGGCAGTC-3'; reverse, 5'-TCGGAAAATGTCATCTTCGATCTCTGGGTTGTC-3'. The wild-type protease plasmid (0.7 ng) was subjected to 30 cycles of PCR to obtain an approximate 1% mutagenesis rate. Subsequently, 500 ng of the resultant PCR products was used as megaprimers to create the library plasmid by a second round of PCR. After overnight *DpnI* treatment, the mutant library was initially transformed into XL10-Gold competent cells, and then the library vectors were extracted and retransformed into *E. coli* BL21(DE3) cells for protein expression. FC-14-solubilized protein fractions were subjected to SDS–PAGE analysis. An autolytic product of NS3_{pro} bands (19.8 kDa) served as an unbiased criterion for separation of mutants into functional and nonfunctional groups compared to the wild type (Figure S4 of the Supporting Information). Truncated protein mutants were ignored in the assay; 103 mutants were selected for further DNA sequencing, which revealed 336 amino acid substitutions, giving a mutational rate of 1.05%. Of those, 230 amino acid variants were found in the nonfunctional group, conferring a higher mutational rate of 1.27%.

Probability of contribution to noncleavage (PCN) scores were assigned to all mutated residues as follows. All mutant sequences were aligned. If a sequence was associated with noncleavage, a probability p was assigned to each mutation in that sequence according to the total number of mutations in the sequence. Thus, if five mutations were found in a sequence, each mutation would receive a p of 0.2. If a particular mutation was also seen in active autolytic data, it was excluded from this procedure. All p values associated with a particular residue were then incorporated into the recursion equation $f(n+1) = f(n)(1 - p_{n+1}) + p_{n+1}$, where $f(0) = p_1$, generating PCN scores for each

alignment column where inactive proteolytic mutations were available.

A sliding window approach was utilized to identify regions of particular importance in autolysis. For a residue of interest, the sum of all PCN scores within a window of ± 7 sequence positions was divided by the total of all cleavage-positive mutations within the same window. The window was then shifted by one sequence position and the process repeated. The resulting ratios are shown on the y-axis of Figure 4B. Given this method, far N- and C-terminal residues are not represented on the graph.

RESULTS

Expression and Solubilization of the Dengue Protease Complex in a Membrane-Anchored Form. Initially, we attempted to express dengue protease complexes of full-length NS2B with NS3 and NS3_{pro} in *E. coli* with traditional amino- or carboxyl-terminal hexahistidine tags with an aim to denature and subsequently refold the recombinant protease from the inclusion body in the presence of a lipid or a detergent. However, the expression level was shown to be very low under various conditions that were tested, and recombinant clones were not genetically stable as the expression ability was occasionally abolished (Figure 1B, lane 9). To overcome difficulties in overexpression and protein folding of the NS2B–NS3 complex, we exploited *B. subtilis* Mistic as a fusion tag (110 amino acids; $M_w = 13$ kDa) for targeting the viral protease to the membrane, and facilitating membrane insertion and protein folding.²⁵ In the pilot phase of the project, we fused dengue NS2B–NS3 and NS2B–NS3_{pro} protease complexes to the C-terminus of Mistic and examined expression levels via SDS–PAGE followed by Western blot analysis. Expression of both NS2B–NS3 and NS2B–NS3_{pro} complexes was drastically boosted by Mistic fusion upon IPTG induction (data not shown). On the basis of these preliminary results, we reconstructed the expression system to be more universal and to prompt the purification process. We designed an expression cassette for membrane protein expression utilizing the pETDuet-1 vector. The resultant plasmid harbored the *Mistic* gene linked to an octahistidine tag flanked by two poly-glycine-serine (GS) linkers, and the thrombin cleavage sequence at its C-terminus (Figure 1A).

We decided to focus on only the NS2B–NS3_{pro} protein precluding the C-terminal helicase domain of NS3 given that the interaction with the NS2B activator protein is likely confined to the protease domain of NS3, and to encourage purification success. On the basis of SDS–PAGE followed by Western blotting with an anti-His tag antibody, the pMHTD–NS2B–NS3_{pro} vector produced a highly stable and comparably high level of expression under most tested conditions with varying culturing temperatures (18–37 °C), IPTG concentrations (10–500 μ M), and types of host strain (BL21, C41, and C43). We defined the optimal expression condition as a 6 h induction with 100 μ M IPTG at 25 °C in BL21(DE3) cells. Under this refined condition, the Mistic-tagged NS2B–NS3_{pro} complex ($M_w = 49.6$ kDa) was expressed in the insoluble fraction as expected for a membrane-integral protein, but this experiment unexpectedly revealed multiple low-molecular mass fragments on the Western blot (Figure 1B). We deduced that these observed fragments could be ascribed to either proteolytic activities or translational dropout. To eliminate the possibility of the translation recess due to incompatible codon usage, we further introduced the pRARE2 plasmid (Novagen) encoding

tRNAs supplied for seven rare codons in *E. coli* into the recombinant strain. Coupling the supplementation of pRARE2 with the addition of a protease inhibitor cocktail (Roche) in the cell lysis buffer weakened some specific bands in the Western blot, thereby improving the purity of the recombinant protein before subsequent purification processes.

We next performed screening of detergents suitable for solubilizing the protease complex from the membrane. Among 17 representative detergents previously reported for membrane protein solubilization and crystallization tested, lauryl dimethylamine oxide (LDAO), cetyltrimethylammonium bromide (CTAB), and FC-10–14 were capable of efficiently solubilizing the protease complex from the membrane (Figure 1C). The CTAB-solubilized protein fraction was, however, labile and heavily precipitated a few hours after protein extraction. It is noted that LDAO was also employed to successfully solubilize Mistic and its fusion proteins in the original work.²⁵ The FC class of detergents indicated a clear relationship between chain length and solubilization yield, with FC-14 showing a >10-fold increase over LDAO. FC-14 is a zwitterionic detergent containing a negatively charged phosphate headgroup with an unbranched hydrophobic tail structurally related to phosphatidylcholine (PC), a natural phospholipid and major constituent of the lipid bilayer of mammalian cells. The FC series have recently proven to be highly useful in solubilization, refolding, and determination of structures of several integral membrane proteins.^{26–28} Its moderate critical micelle concentration (CMC) [0.0046% (w/v)] also allows any subsequent detergent exchange to a milder nonionic such as *n*-dodecyl β -D-maltoside (DDM) during purification with affinity bead immobilization. FC-14 was therefore selected as the optimal solubilization agent for following purification processes.

Purification of the Wild-Type and Mutant Dengue NS2B–NS3_{pro} Protease Complexes. In addition to the wild-type viral protease, two single-amino acid variants of NS3_{pro}, A1E and S135A, were also produced for comparison and further structural analysis (Figure 1B). The A1E mutant has a small alanine residue-specific for position P1' (the amino acid immediately downstream of the cleavage site) being replaced with a bulky glutamate residue; a consequent failure of self-cleavage at the NS2B–NS3 junction (loss of *cis* activity) was previously reported.^{16,29} In contrast, the S135A mutant is a completely inactive protease because of the substitution of the catalytic serine residue in the active site of NS3_{pro} with alanine.³⁰ These two mutants showed protein expression and detergent solubilization behavior equivalent to those of the wild type (Figure 1B). Moreover, the A1E mutant significantly diminished two specific fragments from the affinity-purified proteins, whereas S135A abolished four compared to the wild type (Figure 2A, lanes 8–10). These facts were indicative of two intrinsic internal cleavage sites in the NS2B–NS3_{pro} protein, including the NS2B–NS3 junction. The two 24 and 30 kDa fragments (bands *d* and *e* in Figure 2A and Figure S2 of the Supporting Information), absent in S135A and reduced in A1E mutants, likely represented autolytic cleavage products at the NS2B–NS3 junction resulting in Mistic–NS2B and NS3_{pro} fragments of 29.8 and 19.8 kDa, respectively. An apparent increase in the size of NS3_{pro} on SDS–PAGE was corroborated by previous studies³⁰ and was further confirmed by Western blot analysis with an anti-NS3_{pro} antibody. The recognizable cleavage at the NS2B–NS3 junction in the A1E mutant was unexpected and inconsistent with earlier reports regarding the *in vitro trans* activity of the NS2B_H–NS3_{pro} complex against

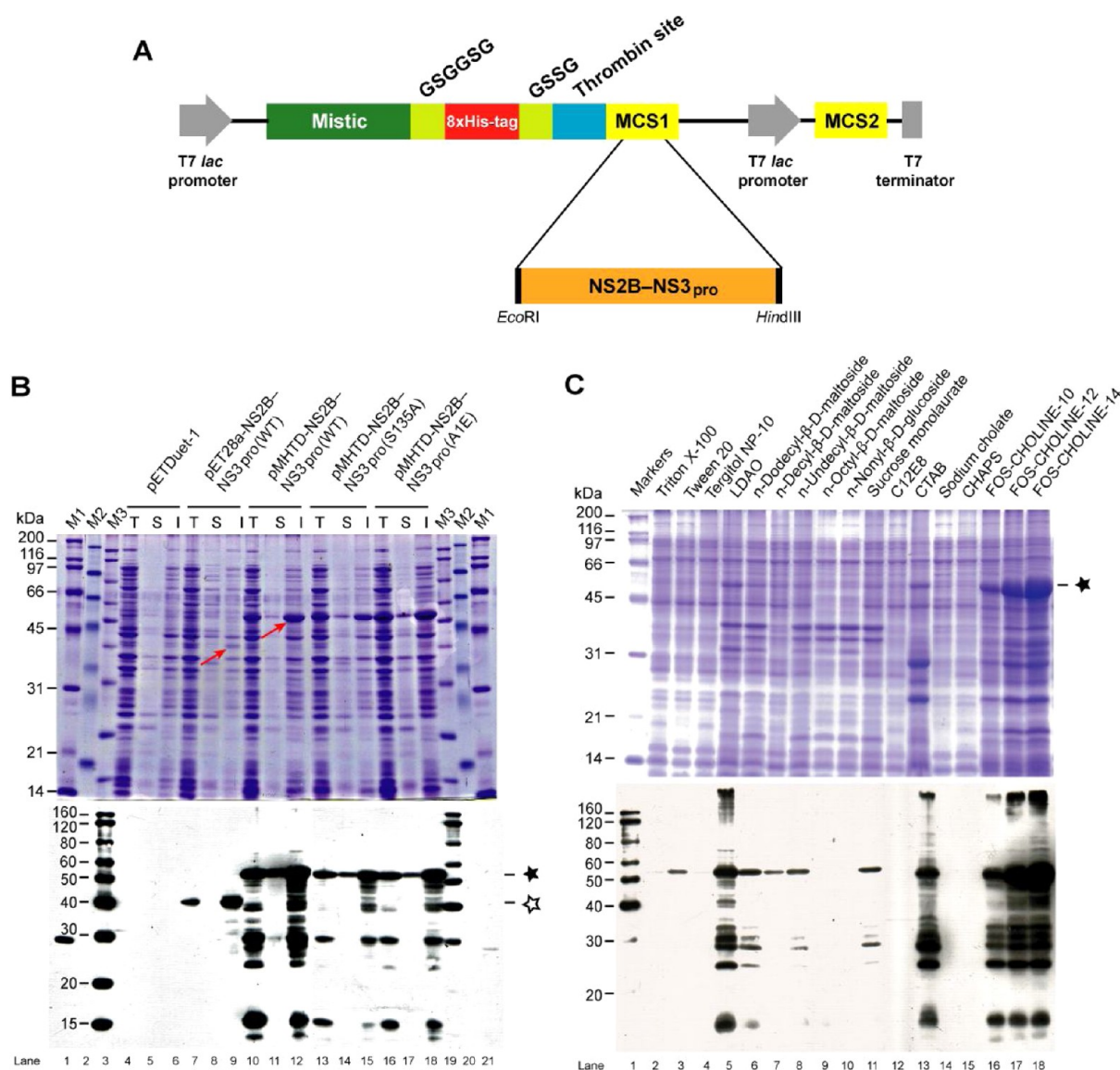


Figure 1. *E. coli* expression and solubilization of the Mistic-fused DENV-2 NS2B-NS3_{pro} complex. (A) Schematic representation of the inducible expression cassette in the pMHTD vector. (B) Protein expression profiling of dengue NS2B-NS3_{pro} complex variants in the BL21(DE3) strain carrying the pRARE2 plasmid. Proteins were stained with Coomassie Blue (top) and further immunoblotted with an anti-His tag antibody (bottom). The total crude cell extracts (T) were fractionated by ultracentrifugation into the supernatant (S) and the pellet (I) containing the cellular membrane. Three protein markers [M1, broad range standards (Bio-Rad); M2, prestained standards (Bio-Rad); M3, BenchMark His-tagged standards (Invitrogen)] were used for comparison in these experiments. It is noted that the level of protein expression of all Mistic-tagged NS2B-NS3_{pro} variants (★, 49.6 kDa) exceeded that of the traditional His-tagged NS2B-NS3 protein (☆, 34.7 kDa, lanes 7–9) by 10-fold (red arrows). (C) Pilot screens of the detergent solubilizing the dengue protease were analyzed via SDS-PAGE (top) and further validated by a Western blot against the His tag (bottom).

synthetic peptide substrates.²⁹ We also ruled out the possibility that these cleavage patterns arose from traces of cellular protease contamination as evidenced by the lack of cleavage products in the S135A mutant, and by the fact that the cleavage sites were consistent with the dengue protease specificity. These results clearly attested to an active form of the recombinant membrane-integral NS2B-NS3_{pro} complex and guaranteed its proper folding in FC-14 (see also Figure 2B).

We also identified a plausible second autolytic cleavage site in NS3_{pro} that produces ~32.9 and ~16.7 kDa fragments by N-terminal Edman degradation sequencing (Figure 2A, bands *c* and *f*, and Figure S3 of the Supporting Information). The cleavage occurred at the KQK²⁸↓G²⁹ site, which closely resembles the NS2B-NS3 junction. A similar report was also

obtained from the recombinant West Nile virus NS2B_H-NS3_{pro} complex;³¹ however, the cleavage at this minor site was not empirically observed *in vivo*.³⁰ The cleavage sequence is located at the border between the end of the first helix and a turning loop of NS3, separated by approximately 20 Å from the active site. Moreover, we could not rule out the possibility that this uncommon cleavage site is less accessible to the protease active site in full-length NS3 than it is in the isolated protease domain. The question of whether this site is targeted by the dengue protease in infected cells, therefore, remains controversial.

Taking advantage of the thrombin recognition sequence embedded in our pMHTD vector, we removed the Mistic and octahistidine tags via an addition of thrombin protease to the

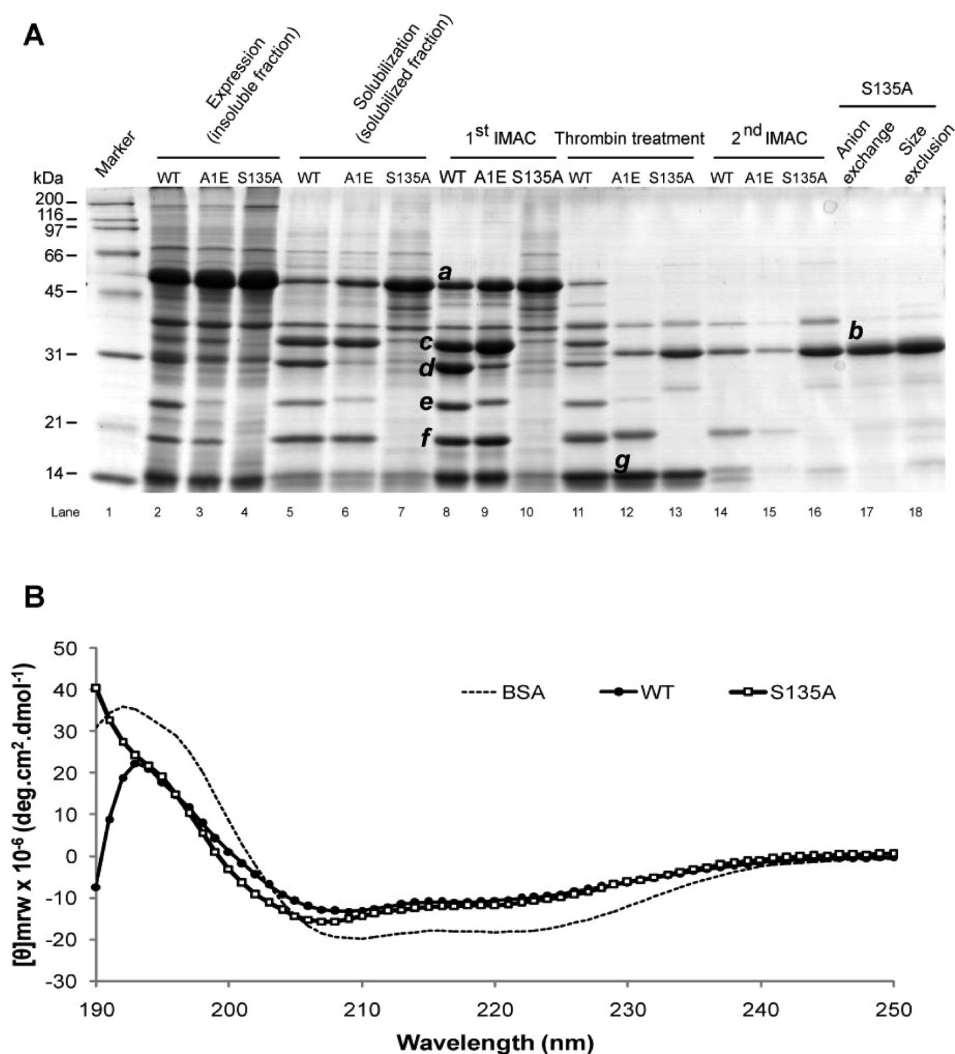


Figure 2. Summary of protein purification. The wild type and two mutants of the NS2B–NS3_{pro} complex were isolated and purified from the *E. coli* membrane in the presence of FC-14 (see details in the Experimental Procedures). Only an inactive S135A mutant was subjected to additional purification by anion exchange (lane 17) and gel filtration (lane 18) columns to improve the purity for further structural analysis. Italic characters denote autolytic fragments corresponding to those proven in Figure S2 of the Supporting Information: *a*, full-length fusion protein (49.6 kDa); *b*, NS2B–NS3_{pro} (34.5 kDa); *c*, Mistic–NS2B–Δ28aa (32.9 kDa); *d*, Mistic–NS2B (29.8 kDa); *e*, NS3_{pro} (19.8 kDa); *f*, NS3_{pro} lacking Δ28aa (16.7 kDa); *g*, Mistic (15.1 kDa). Numbers in parentheses indicate the calculated molecular mass of each protein. Δ28aa represents residues 1–28 at the N-end of NS3_{pro}. (B) Far-UV CD spectra of the wild-type protease complex and S135A mutant displayed principal secondary structure of α -helix comparable to that of bovine serum albumin (BSA). Residue ellipticity $[\theta]$ has units of degrees square centimeters per decimole.

nickel affinity-purified fractions (Figure 2A and Figure S2 of the Supporting Information). In the case of the dengue NS2B–NS3_{pro} complex, we found that a considerable amount of thrombin protease was required for complete digestion. Further tests optimized the concentration at 100 units/mg of protein. It is likely that the optimal length of the linkers flanking the thrombin site is a predominant factor for efficient digestion via exposure of the recognition sequence to the solvent. Furthermore, we also examined alternative cleavage sequences of TEV and HRV 3C proteases, but the results were not superior to those for thrombin (data not shown).

Following digestion, Mistic and uncleaved proteins were trapped via repeated nickel affinity matrix treatment. The flow-through fractions were batched together and analyzed via SDS–PAGE (Figure 2A). During purification steps, it was found that the wild-type protein was progressively autolyzed into specific fragments, and the full-length NS2B–NS3_{pro} complex (34.5 kDa) was difficult to isolate. Addition of several

serine protease inhibitors, including aprotinin, failed to prevent the fragmentation, contrary to a prior report.¹⁷ Therefore, purification of the wild-type NS2B–NS3_{pro} complex was not pursued, and we decided to use the secondary affinity-purified fractions for further enzymatic assays. Meanwhile, the S135A mutant was subjected to subsequent chromatography with anion exchange and size exclusion columns, typically yielding 1.3 mg of protein/L of bacterial growth with a sufficiently high purity (~95%) for further characterization and application to crystallization screening.

NS2B was predicted to be comprised of three or four transmembrane helices with at least one β -strand in the central hydrophilic part, whereas NS3_{pro} mainly consists of β -sheets.¹² When subjected to far-UV CD spectroscopy, the wild-type and S135A NS2B–NS3_{pro} complexes displayed a spectrum characteristic of a predominantly α -helical protein with minima at 208 and 222 nm, compared with the standard BSA (~60% α -helix). The results confirmed the folding of NS2B as a mainly

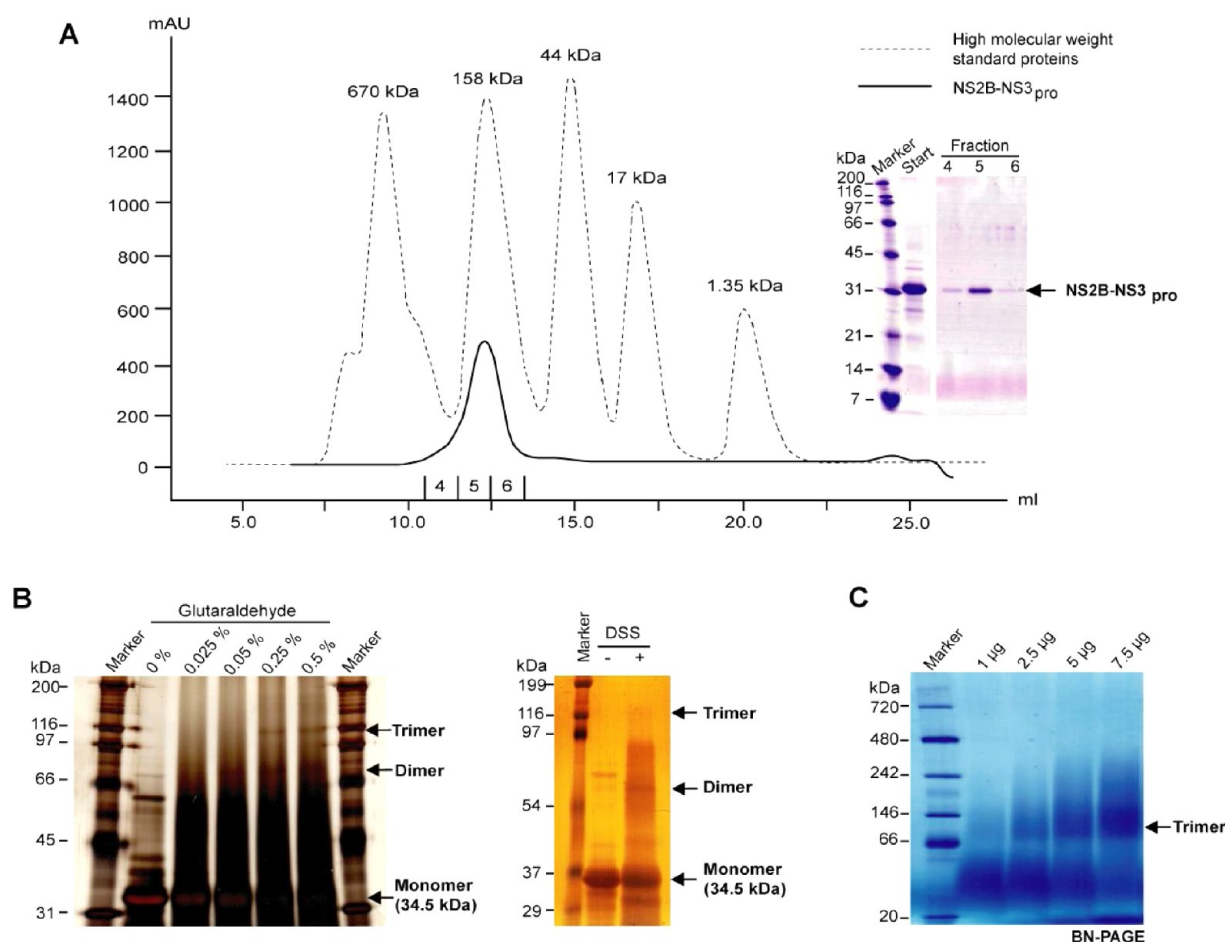


Figure 3. Oligomerization of the purified NS2B-NS3_{pro} complex. (A) Gel filtration analysis of the purified S135A protease mutant run in 0.1% FC-14 on a Superdex 200 HR10/30 column. Absorbance was recorded at 280 nm. The NS2B-NS3_{pro} complex eluted as a detergent-solubilized trimer when compared to the standard proteins (dashed line). The inset shows the result of Coomassie staining following SDS gel electrophoresis of the peak fractions. (B) NS2B-NS3_{pro} complexes were chemically cross-linked with glutaraldehyde (left) and DSS (right) and visualized via silver staining on SDS-PAGE. Both dimeric (69 kDa) and trimeric (103.5 kDa) forms were observed for both cross-linkers. Note that inefficient cross-linking is likely ascribed to a few amino acid residues with amine moieties existing in the transmembrane region of NS2B. (C) The native state of the purified recombinant S135A mutant was analyzed via BN-PAGE. The dengue NS2B-NS3_{pro} complex was detected as an ~100 kDa complex in accordance with increasing amount of protein input.

helical protein (Figure 2B). Moreover, the S135A mutant conceivably evinces a slightly lower ratio of β -strands to helices than the wild type, assigned by the lack of the positive peak at 195 nm, and a minor increase in the size of the negative signal at 208 nm. This may be attributed to local structural changes following the autolytic cleavage of the active enzyme.

Oligomerization State of the Purified NS2B-NS3_{pro} Complex. A single high-molecular mass peak of the NS2B-NS3_{pro} complex was observed via gel filtration profiling. Utilizing protein standards, the apparent mass of the NS2B-NS3_{pro}-detergent complex was estimated to be ~160 kDa (Figure 3A). The micelle size of FC-14 was determined to be 47 kDa,³² indicating that the NS2B-NS3_{pro} protein unit is solubilized in a complex of three monomers (34.5 kDa). To provide strong evidence supporting the gel filtration analysis, we conducted a glutaraldehyde cross-linking experiment with pure S135A protein, followed by analysis via SDS-PAGE [Figure 3B (left panel)]. Although the efficiency of cross-linking was moderate, the results revealed two specific bands of ~69 and 110 kDa identical to the sizes of the dimer and trimer, respectively, according to increasing cross-linker concentration. A similar result was also obtained using DSS as a cross-linker

[Figure 3B (right panel)]. Consistently, the S135A protein migrated as a 100 kDa complex in nondenaturing BN-PAGE (Figure 3C). Taken together, these results naturally led us to a conclusion of the formation of the trimeric NS2B-NS3_{pro} complex.

Random Mutagenesis. To globally identify essential residues and motifs for the autolytic activity of the dengue NS2B-NS3_{pro} complex, we created a PCR-based random mutation library of the dengue NS2B-NS3_{pro} complex and screened for protein mutants that have functionally impaired autolytic activity in an in vitro gel assay. The key to the approach is achieving an appropriate mutagenesis rate. Low rates of mutagenesis require abundant mutants to be cloned and sequenced, whereas a high rate of mutagenesis frequently yields truncated proteins because of the existence of rare or stop codons and also complicates interpretation of the inactivating mutation. To overcome these difficulties, we introduced a new approach by dividing protein mutants into functional and nonfunctional groups and employed a scoring strategy to assess the effects of mutations on activity. Initially, we optimized the PCR condition to yield an average mutagenesis rate of ~1% in the NS2B-NS3_{pro} complex.

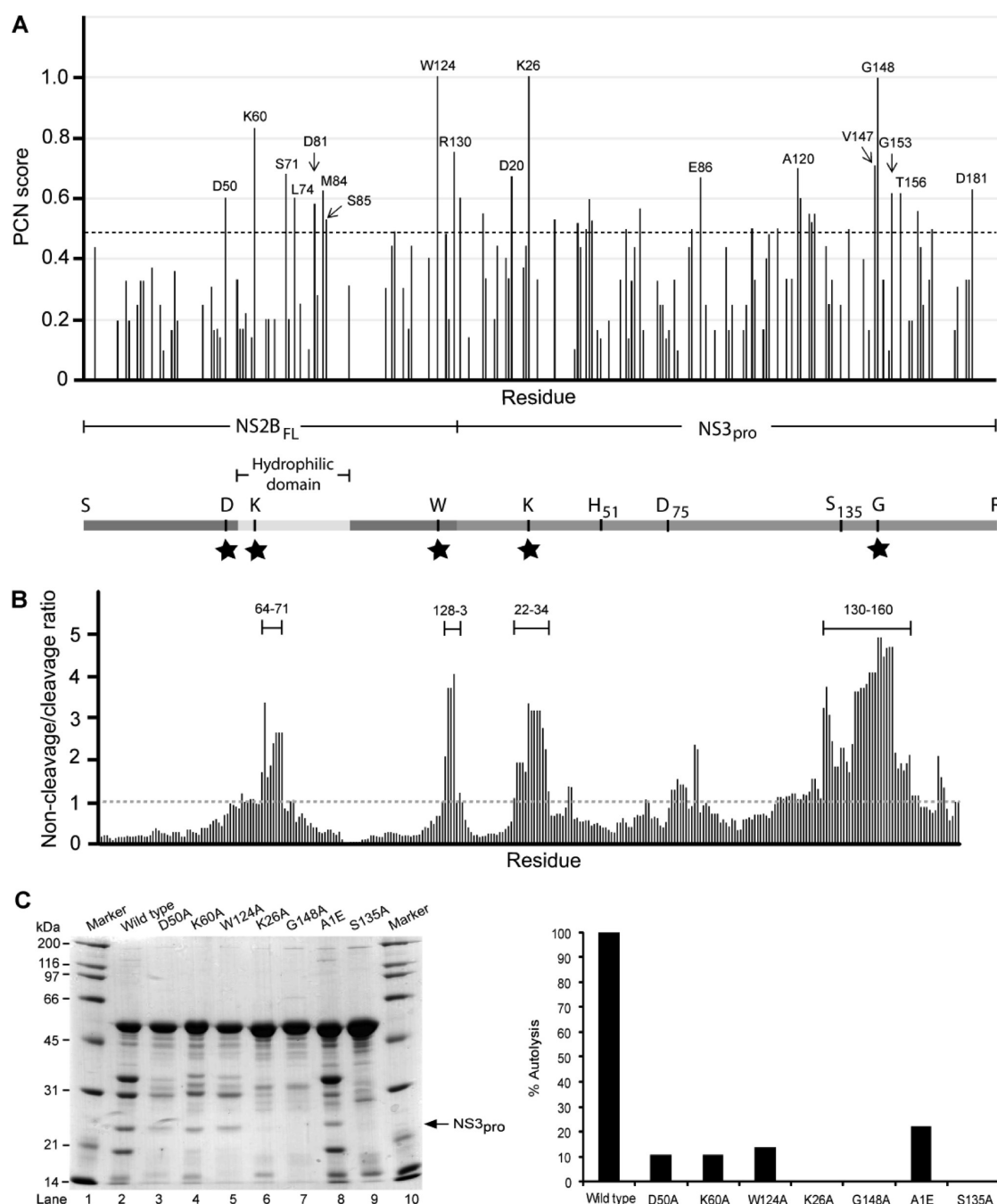


Figure 4. Random mutagenesis studies of the NS2B–NS3_{pro} complex. (A) Each mutated residue was evaluated by a PCN score, and residues giving significant peaks above the cutoff (0.47) are labeled. Five representative residues (★) were selected for further single-alanine mutation analysis. (B) Scan for essential motifs for autolytic activity by a sliding window of 15 amino acids (see Experimental Procedures for details). The mean value (1.02) was used as a cutoff (dotted line). (C) Gel-based autolytic assays of protein mutants. The relative intensities of NS3_{pro} bands (black arrows) were quantitated and are plotted in the right panel.

Individual mutational clones were solubilized and screened on a gel-based assay whereby the sizes of protein mutants were validated and truncated mutants were excluded from the screen (Figure S4 of the Supporting Information). The band of NS3_{pro}, a distinguishable autocleavage product, was used as criterion for the selection of the active and inactive enzymes by comparison with the wild type and S135A, respectively. In total, 103 clones were sequenced, of which 58 represented functionally inactive mutants. There were 230 amino acid substitutions found in 148 of 314 residues of the inactive clones, whereas 106 mutations were found in 68 residues of the

active clones. We note that the appearance of translational termination in mutant proteins was as frequent as 48% in our library screen.

Following the alignment of all mutant sequences, we assigned PCN scores to all residues for which cleavage-negative mutants were seen. This metric integrates data relating to the total number of mutations within sequences and the total number of mutants for any particular residue to offer an estimate of that residue's contribution to noncleavage without using conservation data (see details in Experimental Procedures). The PCN values were plotted (Figure 4A). In several

cases, a PCN value of 1.0, representing certainty that a particular residue is critical for cleavage, is seen. This occurred when the mutagenesis procedure produced only one cleavage-negative mutation in a sequence. As a proof of concept, we performed targeted point mutation analysis of five residues that had particularly high scores. The results clearly revealed that all tested alanine-substituted mutants exhibited impaired autolytic activity compared to the wild-type enzyme, particularly K26A and G148A (Figure 4C). These results confirmed the validity of our analyses and specified five exclusive residues of the membrane-anchored protease complex fundamental for autolytic activity.

Seeking domain-wide motifs of protease activity from the random library, we divided the sums of PCN against sums of cleavage-tolerant mutations with 15 residue windows to obtain ratios indicative of mutation sensitivity (Figures 4B). The results immediately revealed four nonoverlapping regions, including the central hydrophilic region of NS2B, which is involved in the activation of the protease, proving the validity of this approach. The NS2B–NS3 junction-juxtaposed region also showed a high-scoring peak as expected by amino acid sequence-specific recognition and proteolytic cleavage by NS3_{pro}. In NS3_{pro}, two specific regions forming β -hairpins at both ends of the protein indicated crucial roles in autolytic activity. The first N-terminal β -hairpin (residues 22–34) and the C-terminal region including the catalytic Ser¹³⁵ residue and a terminal β -hairpin (residues 130–154) are located in the proximity of the center of the molecule encompassing the active site. Important roles of the C-terminal motifs in NS3_{pro} have been well documented in previous *in vivo* and *in vitro* mutagenesis studies,^{30,33} but the role played by the N-terminal β -hairpin has not yet been described.

DISCUSSION

In this study, we focused on an *E. coli* expression system for high-yield protein production of the dengue protease NS2B–NS3_{pro} complex. Most likely, NS2B causes alteration of membrane topology and possesses cytolytic activity in mammalian cells.^{34,35} Earlier efforts to express and purify the dengue NS2B–NS3_{pro} complex from *E. coli* were performed by renaturation of the misfolded protein from inclusion bodies without the use of lipid or detergent, implying that those recombinants were likely not to be properly folded.³⁶ By varying different available tags, we found that only Mystic could accelerate the expression level of the NS2B–NS3_{pro} complex to be sufficient for further structural and functional analyses. The advantage of the Mystic tag likely involves the successful N-terminal signal-independent membrane trafficking, which in turn promotes proper folding and circumvents host protein degradation machinery. The only difficulty we encountered during the purification processes was in removing the entire Mystic and His tag region by proteolytic digestion. Increasing the length of two specific GS linkers might have provided more accessibility of the cleavage site, which results in an extra N-tail after removal. Moreover, it has generally been supposed that the linker also renders a sufficient space between Mystic and the protein of interest, which possibly contributes to expression success and proper folding.²⁵

The isolated inactive S135A mutant protein that was solubilized and stabilized in detergent FC-14 proved to be highly pure and formed a monodisperse trimer on gel filtration analysis (Figure 3A). Very recently, Huang et al. reported the expression and purification of dengue NS2B alone from *E. coli*

inclusion bodies via the refolding with lysomyristoylphosphatidylglycerol (LMPG). It is noted that the size and chemical structure of the LMPG detergent closely resemble those of FC-14 used in our study.³⁷ Oligomerization of NS3_{pro} was not observed in previous studies,^{12,38} thus suggesting that the intact NS2B is likely responsible for the trimeric assembly in the membrane. Although the existence of the NS2B–NS3_{pro} trimer in dengue-infected cells is so far uncharacterized, roles possibly played by trimerization in viral protein maturation cannot be ruled out. Potential support for this trimeric model is offered in known crystal structures, where the N-terminus of NS3_{pro} is folded back onto the opposite side of its active site, implying a *trans* cleavage mode of autolytic activity. It is thus not preposterous to speculate that NS2B–NS3_{pro} junctions are cleaved by the neighboring protomer in the trimeric molecule; however, the hypothesis may require further biochemical and structural work on the intact NS2B–NS3_{pro} complex in the membrane.

The solubilized NS2B–NS3_{pro} complex exhibited functional activity of autoproteolytic cleavage in the FC-14 micelle that mimics the cellular environment of the mammalian bilayer membrane. The autolytic activity was scarcely affected by the fusion of the Mystic tag, suggesting that Mystic barely disturbs the folding of the fused membrane protein in our constructs. This observation allowed a throughput gel screening of autolytic activities of the mutation library without purification. Our random mutagenesis studies demonstrated four regions crucial for the protease activity of the NS2B–NS3_{pro} complex in an unbiased manner. To provide a more comprehensive view of the intact viral protease, we have created a complete model of the active DENV-2 NS2B_H–NS3_{pro} complex by accurately aligning and combining three known crystal structures.^{12,39,40} During the revision of our manuscript, a new catalytically active, closed conformation of the DENV-3 protease structures became available.⁴¹ In the active structure of the NS2B_H–NS3_{pro} complex bound to the substrate peptide Bz-nKRR-H (Protein Data Bank entry 3U1I), the P1' residue of the cleavage junction is separated by >20 Å from the active site, thus precluding the possibility of a *cis* autocleavage mechanism. Together with our findings, intermolecular *trans* cleavage in the trimeric assembly seems more feasible.

On the basis of hydrophobicity analysis and the prediction of transmembrane segments of NS2B, residues Arg⁴⁷–Tyr⁹⁶ constitute the cytoplasmic domain of NS2B, which is well corroborated by an earlier finding.¹³ Residues 51–57 of NS2B make an antiparallel sheet with strand β 1 of NS3_{pro} involved in the folding of the protease core. However, this region is less conserved among orthologues relative to its sequence context (Figure S1 of the Supporting Information). We found that the sequences flanking β 1 are important for autolytic activity (Figure 4B). Lys⁶⁰ showed a high PCN score, and the corresponding alanine-substituted mutant (S61A) was inactive *in vitro* for the WNV enzyme.⁴² The other region giving significant PCN in NS2B encompasses residues 74–85, with its important role in activating protease activity having been described by mutational studies of both DENV-2 and WNV.^{14,42} This region constructs a β -hairpin observed in both recent structures of DENV and WNV protease complexes but in different conformations.^{39–41} This β -hairpin is inserted into NS3_{pro} between β 10 and β 14 forming a β -barrel comprised of β 10, β 11, β 14, and β 15; however, direct interactions between the β -hairpin and the cleavage substrate are not essential. Therefore, NS2B_H directly activates the protease activity by

refolding the protease domain upon β -strand insertions, which in turn constrain the active site and indirectly contribute to the recognition of the substrate sequence.

It is likely that the active site of NS3_{pro} is anchored to or in the proximity of the membrane. The lipids should obscure accessibility to the active site or may play an unknown role in substrate selectivity. The protease inhibitor aprotinin in the complex structure with NS3_{pro}⁴¹ completely overlaps with the bilayer membrane in our dengue model, supporting our result that aprotinin failed to inhibit autolytic activity during purification. Defective autocleavage of NS2B mutant W124A can be attributed to failure to efficiently locate the cleavage junction in the active site. Therefore, interactions with the membrane may have a strong impact on the activity and substrate selectivity of NS3_{pro}¹⁵. The *in vivo trans* cleavage activity of the NS2B–NS3 complex is confined to the NS protein boundaries exclusively on the cytosolic side of the ER membrane, and to the best of our knowledge, there is yet no evidence of NS2B–NS3 complex-catalyzed cleavage of host proteins, a large number of which should contain the classic cleavage sequence in infected cells. Because most *in vitro* characterizations of the NS2B–NS3_{pro} complex have so far been achieved in solution using an engineered enzyme with synthetic model substrates, special caution is thus required in extrapolating prior results to the physiological membranous environment.

We also clarified two structural elements of NS3_{pro} that are important for autolytic activity. The β 12– β 13 hairpin at the C-terminus of NS3_{pro} is highly conserved (Figure S1 of the Supporting Information) and has been well characterized by *in vivo* and *in vitro* mutagenesis studies.^{30,33,43} In contrast, the contribution of the first β 1– β 2 hairpin is not known. While the region is less conserved, the K26A NS3_{pro} mutant completely abolished autolytic activity in a fashion similar to that of the well-studied G148A³⁰ (Figure 4C). Strand β 1 makes a specific interaction with β a of NS2B_H, thus involving the activation of protease activity in the refolding process. Moreover, β 2 is located close to the substrate-binding site, and residues 30–34 form the hydrophobic P4' pocket for the recognition of the substrate in NS3_{pro}⁴¹.

High degrees of conservation are seen in the β 3– α 1 region, which includes the crucial His⁵¹ residue at the catalytic center. It is notable, therefore, that a number of mutations in this region did not affect autocleavage. For example, Trp⁵⁰ is perfectly conserved among Flaviviridae (Figure S1B of the Supporting Information); however, three sequences with W50R mutations showed unaltered cleavage activity in our screen. The disparity between the high levels of conservation and insensitivity to cleavage-abolishing mutations could possibly be explained by positing a second crucial function for this region (e.g., interdomain interaction).

Our protein preparation provides a promising avenue for future crystallographic studies of viral proteases in the membrane-bound form and in the search for specific therapeutic inhibitors. Our random mutagenesis results cover all previous mutational studies and revealed fundamental structural elements not characterized previously. The methodology can be generally applied to globally define essential motifs in enzymes without traditional alanine scanning. We propose here that the membrane plays roles in the positioning and recognition of the actual peptide substrate by NS3_{pro}, and therefore, the design of effective inhibitors must await further

structural determination of the intact membrane-anchored NS2B–NS3_{pro} complex.

■ ASSOCIATED CONTENT

Supporting Information

Amino acid sequence alignments of the flavivirus NS2B–NS3 complex (Figure S1), assessment of thrombin digestion for removal of Mistic (Figure S2), N-terminal Edman degradation sequencing of autolytic products (Figure S3), and the gel-based activity screen of the NS2B–NS3_{pro} mutant library (Figure S4). This material is available free of charge via the Internet at <http://pubs.acs.org>.

■ AUTHOR INFORMATION

Corresponding Author

*Address: 25/25 Phutthamonthon 4 Rd., Salaya, Nakhon Pathom, Thailand 73170. Telephone: +66 2 441 9004, ext. 1468. Fax: +66 2 441 9906. E-mail: mbscr@mahidol.ac.th.

Funding

This work was supported in part by Grants MRG5180197 (to S.C.) and BRG4980008 (to G.K.) from the Thailand Research Fund and a Grant-in-Aid from Mahidol University. O.C. was supported by a scholarship from the Thailand Graduate Institute of Science and Technology (TGIST 01-S2-023).

Notes

The authors declare no competing financial interest.

■ ACKNOWLEDGMENTS

We thank Ui Okada (Graduate School of Life Sciences, Hokkaido University, Sapporo, Japan) for cloning the *Mistic* gene from *B. subtilis* and Bunpote Siridechadilok (National Center for Genetic Engineering and Biotechnology, Pathumthani, Thailand) for kindly providing the anti-NS3_{pro} antibody, glutaraldehyde, and gel filtration standards.

■ ABBREVIATIONS

DENV, dengue virus; NS2B and NS3, viral nonstructural proteins 2B and 3, respectively; NS3_{pro}, N-terminal protease domain of the NS3 protein; NS2B_H, central hydrophilic activation peptide of the NS2B protein; MCS, multicloning site; GS linker, poly-glycine-serine linker; CMC, critical micelle concentration; FC, fos-choline detergent.

■ REFERENCES

- (1) World Health Organization (WHO) (2009) Dengue and Dengue Haemorrhagic Fever. Fact Sheet 117, WHO, Geneva.
- (2) Gubler, D. J. (1998) Dengue and dengue hemorrhagic fever. *Clin. Microbiol. Rev.* 11, 480–496.
- (3) Halstead, S. B. (2007) Dengue. *Lancet* 370, 1644–1652.
- (4) Murray, C. L., Jones, C. T., and Rice, C. M. (2008) Architects of assembly: Roles of Flaviviridae non-structural proteins in virion morphogenesis. *Nat. Rev. Microbiol.* 6, 699–708.
- (5) Bollati, M., Alvarez, K., Assenberg, R., Baronti, C., Canard, B., Cook, S., Coutard, B., Decroly, E., de Lamballerie, X., Gould, E. A., Grard, G., Grimes, J. M., Hilgenfeld, R., Jansson, A. M., Malet, H., Mancini, E. J., Mastrangelo, E., Mattevi, A., Milani, M., Moureau, G., Neyts, J., Owens, R. J., Ren, J., Selisko, B., Speroni, S., Steuber, H., Stuart, D. I., Unge, T., and Bolognesi, M. (2010) Structure and functionality in flavivirus NS-proteins: Perspectives for drug design. *Antiviral Res.* 87, 125–148.
- (6) Chambers, T. J., Hahn, C. S., Galler, R., and Rice, C. M. (1990) Flavivirus genome organization, expression, and replication. *Annu. Rev. Microbiol.* 44, 649–688.

- (7) Falgout, B., Pethel, M., Zhang, Y. M., and Lai, C. J. (1991) Both nonstructural proteins NS2B and NS3 are required for the proteolytic processing of dengue virus nonstructural proteins. *J. Virol.* 65, 2467–2475.
- (8) Falgout, B., and Markoff, L. (1995) Evidence that flavivirus NS1-NS2A cleavage is mediated by a membrane-bound host protease in the endoplasmic reticulum. *J. Virol.* 69, 7232–7243.
- (9) Yusof, R., Clum, S., Wetzel, M., Murthy, H. M., and Padmanabhan, R. (2000) Purified NS2B/NS3 serine protease of dengue virus type 2 exhibits cofactor NS2B dependence for cleavage of substrates with dibasic amino acids in vitro. *J. Biol. Chem.* 275, 9963–9969.
- (10) Bartelma, G., and Padmanabhan, R. (2002) Expression, purification, and characterization of the RNA 5'-triphosphatase activity of dengue virus type 2 nonstructural protein 3. *Virology* 299, 122–132.
- (11) Lescar, J., Luo, D., Xu, T., Sampath, A., Lim, S. P., Canard, B., and Vasudevan, S. G. (2008) Towards the design of antiviral inhibitors against flaviviruses: The case for the multifunctional NS3 protein from dengue virus as a target. *Antiviral Res.* 80, 94–101.
- (12) Erbel, P., Schiering, N., D'Arcy, A., Renatus, M., Kroemer, M., Lim, S. P., Yin, Z., Keller, T. H., Vasudevan, S. G., and Hommel, U. (2006) Structural basis for the activation of flaviviral NS3 proteases from dengue and West Nile virus. *Nat. Struct. Mol. Biol.* 13, 372–373.
- (13) Falgout, B., Miller, R. H., and Lai, C. J. (1993) Deletion analysis of dengue virus type 4 nonstructural protein NS2B: Identification of a domain required for NS2B-NS3 protease activity. *J. Virol.* 67, 2034–2042.
- (14) Niyomrattanakit, P., Winoyanu Wattikun, P., Chanprapaph, S., Angsuthanasombat, C., Panyim, S., and Katzenmeier, G. (2004) Identification of residues in the dengue virus type 2 NS2B cofactor that are critical for NS3 protease activation. *J. Virol.* 78, 13708–13716.
- (15) Clum, S., Ebner, K. E., and Padmanabhan, R. (1997) Cotranslational membrane insertion of the serine proteinase precursor NS2B-NS3(Pro) of dengue virus type 2 is required for efficient in vitro processing and is mediated through the hydrophobic regions of NS2B. *J. Biol. Chem.* 272, 30715–30723.
- (16) Li, J., Lim, S. P., Beer, D., Patel, V., Wen, D., Tumanut, C., Tully, D. C., Williams, J. A., Jiricek, J., Priestle, J. P., Harris, J. L., and Vasudevan, S. G. (2005) Functional profiling of recombinant NS3 proteases from all four serotypes of dengue virus using tetrapeptide and octapeptide substrate libraries. *J. Biol. Chem.* 280, 28766–28774.
- (17) Leung, D., Schroder, K., White, H., Fang, N. X., Stoermer, M. J., Abbenante, G., Martin, J. L., Young, P. R., and Fairlie, D. P. (2001) Activity of recombinant dengue 2 virus NS3 protease in the presence of a truncated NS2B co-factor, small peptide substrates, and inhibitors. *J. Biol. Chem.* 276, 45762–45771.
- (18) Miller, S., and Krijnse-Locker, J. (2008) Modification of intracellular membrane structures for virus replication. *Nat. Rev. Microbiol.* 6, 363–374.
- (19) Westaway, E. G., Mackenzie, J. M., Kenney, M. T., Jones, M. K., and Khromykh, A. A. (1997) Ultrastructure of Kunjin virus-infected cells: Colocalization of NS1 and NS3 with double-stranded RNA, and of NS2B with NS3, in virus-induced membrane structures. *J. Virol.* 71, 6650–6661.
- (20) Brinkworth, R. I., Fairlie, D. P., Leung, D., and Young, P. R. (1999) Homology model of the dengue 2 virus NS3 protease: Putative interactions with both substrate and NS2B cofactor. *J. Gen. Virol.* 80 (Part 5), 1167–1177.
- (21) Luo, D., Xu, T., Hunke, C., Gruber, G., Vasudevan, S. G., and Lescar, J. (2008) Crystal structure of the NS3 protease-helicase from dengue virus. *J. Virol.* 82, 173–183.
- (22) Chernov, A. V., Shiryayev, S. A., Aleshin, A. E., Ratnikov, B. I., Smith, J. W., Liddington, R. C., and Strongin, A. Y. (2008) The two-component NS2B-NS3 proteinase represses DNA unwinding activity of the West Nile virus NS3 helicase. *J. Biol. Chem.* 283, 17270–17278.
- (23) Frick, D. N., Rypma, R. S., Lam, A. M., and Gu, B. (2004) The nonstructural protein 3 protease/helicase requires an intact protease domain to unwind duplex RNA efficiently. *J. Biol. Chem.* 279, 1269–1280.
- (24) Rajagopal, V., Gurjar, M., Levin, M. K., and Patel, S. S. (2010) The protease domain increases the translocation stepping efficiency of the hepatitis C virus NS3–4A helicase. *J. Biol. Chem.* 285, 17821–17832.
- (25) Roosild, T. P., Greenwald, J., Vega, M., Castronovo, S., Riek, R., and Choe, S. (2005) NMR structure of Mistic, a membrane-integrating protein for membrane protein expression. *Science* 307, 1317–1321.
- (26) Gorzelle, B. M., Nagy, J. K., Oxenoid, K., Lonzer, W. L., Cafiso, D. S., and Sanders, C. R. (1999) Reconstitutive refolding of diacylglycerol kinase, an integral membrane protein. *Biochemistry* 38, 16373–16382.
- (27) Bass, R. B., Strop, P., Barclay, M., and Rees, D. C. (2002) Crystal structure of *Escherichia coli* MscS, a voltage-modulated and mechanosensitive channel. *Science* 298, 1582–1587.
- (28) Kaiser, L., Graveland-Bikker, J., Steuerwald, D., Vanberghem, M., Herlihy, K., and Zhang, S. (2008) Efficient cell-free production of olfactory receptors: Detergent optimization, structure, and ligand binding analyses. *Proc. Natl. Acad. Sci. U.S.A.* 105, 15726–15731.
- (29) Shiryayev, S. A., Kozlov, I. A., Ratnikov, B. I., Smith, J. W., Lebl, M., and Strongin, A. Y. (2007) Cleavage preference distinguishes the two-component NS2B-NS3 serine proteinases of Dengue and West Nile viruses. *Biochem. J.* 401, 743–752.
- (30) Valle, R. P., and Falgout, B. (1998) Mutagenesis of the NS3 protease of dengue virus type 2. *J. Virol.* 72, 624–632.
- (31) Shiryayev, S. A., Ratnikov, B. I., Chekanov, A. V., Sikora, S., Rozanov, D. V., Godzik, A., Wang, J., Smith, J. W., Huang, Z., Lindberg, I., Samuel, M. A., Diamond, M. S., and Strongin, A. Y. (2006) Cleavage targets and the D-arginine-based inhibitors of the West Nile virus NS3 processing proteinase. *Biochem. J.* 393, 503–511.
- (32) Strop, P., and Brunger, A. T. (2005) Refractive index-based determination of detergent concentration and its application to the study of membrane proteins. *Protein Sci.* 14, 2207–2211.
- (33) Salaemae, W., Junaid, M., Angsuthanasombat, C., and Katzenmeier, G. (2010) Structure-guided mutagenesis of active site residues in the dengue virus two-component protease NS2B-NS3. *J. Biomed. Sci.* 17, 68.
- (34) Ramanathan, M. P., Chambers, J. A., Pankhong, P., Chattergoon, M., Attatippaholkun, W., Dang, K., Shah, N., and Weiner, D. B. (2006) Host cell killing by the West Nile Virus NS2B-NS3 proteolytic complex: NS3 alone is sufficient to recruit caspase-8-based apoptotic pathway. *Virology* 345, 56–72.
- (35) Liu, L., Tian, Y., Gao, N., Chen, Z., Zhang, H., and An, J. (2010) Application of antibodies against nonstructural protein 2B of dengue serotype 2 virus induced by DNA immunisation or recombinant protein NS 2B immunisation in BALB/c mice. *J. Virol. Methods* 163, 10–16.
- (36) Khumthong, R., Angsuthanasombat, C., Panyim, S., and Katzenmeier, G. (2002) In vitro determination of dengue virus type 2 NS2B-NS3 protease activity with fluorescent peptide substrates. *J. Biochem. Mol. Biol.* 35, 206–212.
- (37) Huang, Q., Chen, A. S., Li, Q., and Kang, C. (2011) Expression, purification, and initial structural characterization of nonstructural protein 2B, an integral membrane protein of Dengue-2 virus, in detergent micelles. *Protein Expression Purif.* 80, 169–175.
- (38) Luo, D., Wei, N., Doan, D. N., Paradkar, P. N., Chong, Y., Davidson, A. D., Kotaka, M., Lescar, J., and Vasudevan, S. G. (2010) Flexibility between the protease and helicase domains of the dengue virus NS3 protein conferred by the linker region and its functional implications. *J. Biol. Chem.* 285, 18817–18827.
- (39) Chandramouli, S., Joseph, J. S., Daudenarde, S., Gatchalian, J., Cornillez-Ty, C., and Kuhn, P. (2010) Serotype-specific structural differences in the protease-cofactor complexes of the dengue virus family. *J. Virol.* 84, 3059–3067.
- (40) Aleshin, A. E., Shiryayev, S. A., Strongin, A. Y., and Liddington, R. C. (2007) Structural evidence for regulation and specificity of flaviviral proteases and evolution of the Flaviviridae fold. *Protein Sci.* 16, 795–806.

- (41) Noble, C. G., Seh, C. C., Chao, A. T., and Shi, P. Y. (2012) Ligand-bound structures of the dengue virus protease reveal the active conformation. *J. Virol.* 86, 438–446.
- (42) Chappell, K. J., Stoermer, M. J., Fairlie, D. P., and Young, P. R. (2008) Mutagenesis of the West Nile virus NS2B cofactor domain reveals two regions essential for protease activity. *J. Gen. Virol.* 89, 1010–1014.
- (43) Chappell, K. J., Nall, T. A., Stoermer, M. J., Fang, N. X., Tyndall, J. D., Fairlie, D. P., and Young, P. R. (2005) Site-directed mutagenesis and kinetic studies of the West Nile Virus NS3 protease identify key enzyme-substrate interactions. *J. Biol. Chem.* 280, 2896–2903.